



# Post-Mortem MRI and Histopathology in Neurologic Disease: A Translational Approach

Laura E. Jonkman<sup>1</sup> · Boyd Kenkhuis<sup>2,3</sup> · Jeroen J. G. Geurts<sup>1</sup> · Wilma D. J. van de Berg<sup>1</sup>

Received: 27 June 2018 / Accepted: 29 October 2018 / Published online: 21 February 2019  
© Shanghai Institutes for Biological Sciences, CAS 2019

**Abstract** In this review, combined post-mortem brain magnetic resonance imaging (MRI) and histology studies are highlighted, illustrating the relevance of translational approaches to define novel MRI signatures of neuropathological lesions in neuroinflammatory and neurodegenerative disorders. Initial studies combining post-mortem MRI and histology have validated various MRI sequences, assessing their sensitivity and specificity as diagnostic biomarkers in neurologic disease. More recent studies have focused on defining new radiological (bio)markers and implementing them in the clinical (research) setting. By combining neurological and neuroanatomical expertise with radiological development and pathological validation, a cycle emerges that allows for the discovery of novel MRI biomarkers to be implemented *in vivo*. Examples of this cycle are presented for multiple sclerosis, Alzheimer's disease, Parkinson's disease, and traumatic brain injury. Some applications have been shown to be successful, while others require further validation. In conclusion, there is much to explore with post-mortem MRI and histology studies, which can eventually be of high relevance for clinical practice.

**Keywords** MRI · Histology · Biomarkers · Multiple sclerosis · Alzheimer's disease · Parkinson's disease

## Introduction

Magnetic resonance imaging (MRI) is routinely used in clinical practice to evaluate brain anatomy and pathology in neuroinflammatory and neurodegenerative disorders, to aid (differential) diagnosis or assess disease severity, e.g. estimating atrophy in Alzheimer's disease (AD) or lesion load in multiple sclerosis (MS). Knowledge of the histopathological substrate of these radiological findings can come with a delay; an *in-vivo* MRI is made, and only after death (months or years later) can radiological findings be validated at pathological inspection [1–4]. With the emergence of post-mortem MRI with subsequent histopathological validation of the same donor brain, this delay is no longer a hurdle and various MRI sequences can be assessed for their pathological sensitivity and specificity (Fig. 1 in blue) [5–7].

Importantly, combined post-mortem MRI and histopathology can be used beyond mere validation. It can aid the development of new MRI sequences to detect more subtle pathology *in-vivo* (Fig. 1 in orange), and address more complicated differential diagnosis conundrums, e.g. differentiating Parkinson's disease (PD) from other parkinsonisms [8]. An interplay emerges between clinical practice, radiological development, and pathological validation, to eventually establish a sensitive and specific radiological diagnostic or prognostic biomarker that can be implemented in the clinical and research settings (Fig. 1).

This review focuses on studies using post-mortem MRI and histopathology, working towards the clinical

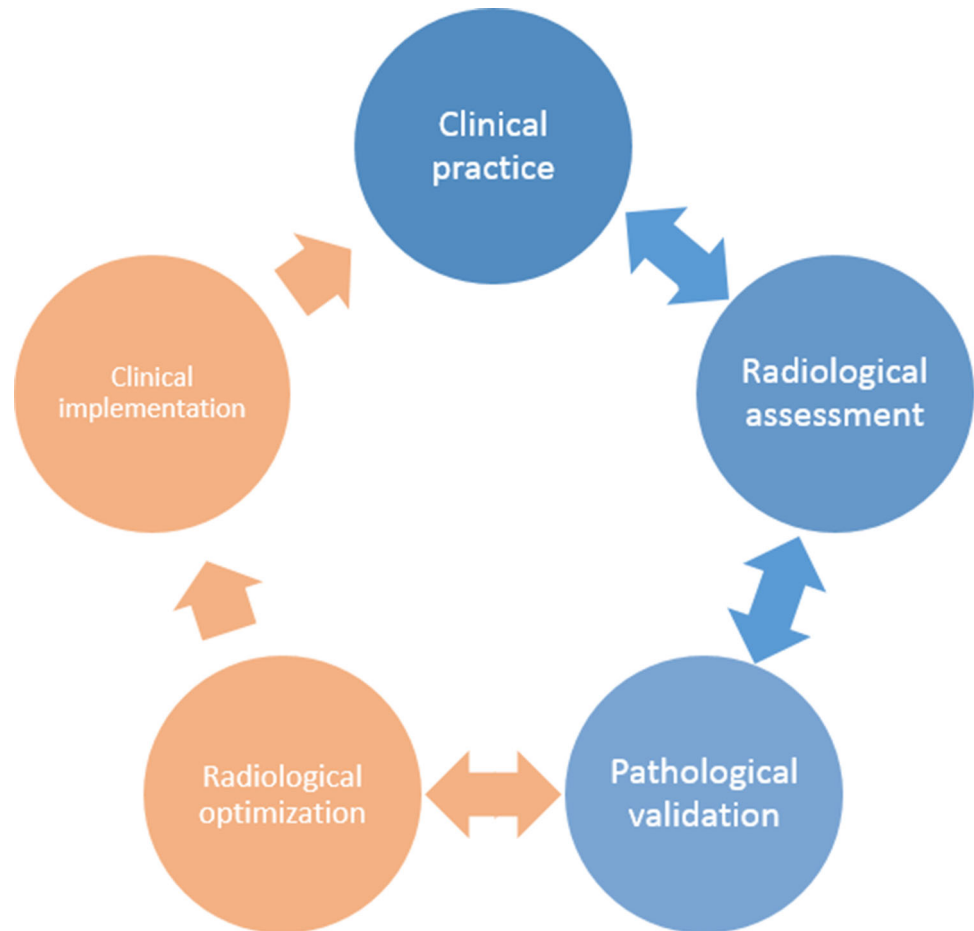
✉ Laura E. Jonkman  
le.jonkman@vumc.nl

<sup>1</sup> Department of Anatomy and Neurosciences, Amsterdam Neuroscience, Amsterdam UMC, Vrije Universiteit Amsterdam, De Boelelaan 1117, Amsterdam, The Netherlands

<sup>2</sup> Department of Human Genetics, Leiden University Medical Center, Leiden, The Netherlands

<sup>3</sup> Department of Radiology, Leiden University Medical Center, Leiden, The Netherlands

**Fig. 1** Cycle for integration of radiological and pathological development into clinical research and practice. Clinical practice uses radiological assessment (MRI) to assess structural brain changes in patients with neuroinflammatory and neurodegenerative disorders. Initial post-mortem MRI and histopathological studies focus on validating MRI sequences for their pathological sensitivity and specificity (blue). However, more recent studies have focused on optimizing and developing MRI sequences to define more sensitive measures to improve diagnostic and prognostic diagnosis in the clinical setting (orange). As such, post-mortem MRI is of high interest to translate MRI features into histopathological terms but also to translate knowledge on the type or distribution of pathological lesions to MRI, thereby integrating clinical practice, radiological development, and pathological validation to establish optimal radiological biomarkers.



applicability of novel MRI biomarkers of neuropathological lesions. First, we discuss the essentials and logistics of setting up an efficient post-mortem MRI and histology pipeline. Then we highlight examples of combined post-mortem MRI and histopathology studies in four neurological diseases—MS, AD, PD, and traumatic brain injury (TBI)—with regards to where they are in the cycle of validation and clinical research implementation.

### Post-mortem MRI and Histopathology Pipeline

Donors for post-mortem brain research are generally recruited through brain banks or body bequest programs after informed consent of the donor for brain autopsy and use of material for research purposes. All procedures of the brain bank have to be approved by a local Medical Ethics Committee. To maintain a high quality of tissue integrity, a short post-mortem interval (time between death and formalin fixation) is crucial. When *in situ* post-mortem MRI (brain still in cranium) or *ex vivo* MRI with fresh tissue is added to the equation, this may pose an extra

challenge. Therefore, an adequate logistic setup is required to prevent unnecessary delays.

The logistics regarding brain autopsy programs without MRI have been described [9–12]. We briefly describe the procedures when both *in situ* and *ex vivo* MRI are included in the protocol, as done by the Normal Aging Brain collection Amsterdam (<http://nabca.eu>), an initiative of the department of Anatomy and Neurosciences of Amsterdam UMC - location VUmc, which includes non-neurological donors, and neurological donors in close collaboration with the Netherlands Brain Bank (<http://brainbank.nl>). This pipeline is based on the Amsterdam protocol as previously described for MS research [13].

After death, the donor is transported to the mortuary of the hospital. There, a team consisting of an MRI researcher and autopsy assistant transport the donor to the MRI scanner and include various conventional and advanced MRI sequences. Upon return to the mortuary, a neuropathologist and an autopsy assistant perform the craniotomy and subsequent brain dissection according to a strict standardized protocol. At this time, only the left hemisphere is dissected and tissue blocks are snap-frozen in liquid nitrogen to allow subsequent genetic, molecular,

and biochemical analysis. The right hemisphere is immersed in 4% buffered formalin for four weeks, after which it is scanned *ex vivo* at 7T. After this ultra-high field MRI scan, the right hemisphere is dissected according to the Brain Net Europe protocol [9] and tissue blocks are embedded in paraffin. A selection of these blocks is used for a comprehensive neuropathological assessment of lesions defining various neurological diseases, such as subtypes of dementia, PD, and MS. Patient data, including demographics, medical history, radiological and neuropathological information, are combined in a donor report.

Additions to this protocol may occur, for instance by means of an *ex vivo* scan of brain slices after craniotomy, upon which MRI-guided tissue dissection can take place (as in MS donors for dissection of specific lesions [13]). Another option is to obtain formalin-fixed brain slices or tissue blocks at autopsy, and use them for ultra-high MRI at a later stage. After embedding, the brain tissue can be stained for a range of immuno- and histochemical markers to assess correlations between MRI signal intensities and morphometric or pathological changes.

In research studies, regions of interest are generally marked on MRI, and histological sections are matched to the corresponding MRI plane, using as many anatomical landmarks (border of the white matter (WM) and gray matter (GM), sulci, gyri, and ventricles) as available. Alternatively, MRI atlases can be used or designed, depending on the research question.

## Post-mortem MRI and Histology in MS

MS is characterized by multifocal lesions in the WM, GM, hippocampus, cerebellum, deep grey nuclei, and spinal cord. These lesions have various degrees of inflammation, demyelination, and other histopathological characteristics [14, 15]. MRI has contributed considerably to the understanding and early diagnosis of MS and is routinely used to monitor the course and progression of disease [16, 17]. Since the early 2000s, post-mortem MRI in MS has also contributed to the interpretation of MRI abnormalities with respect to their underlying histopathology in both WM and GM. We address these findings below.

### WM Lesions and Remyelination in MS

WM lesions in MS are generally readily visible on conventional MRI (e.g. (gadolinium-)T1, T2, and proton-density). However, lesion stage, specifically remyelination, cannot be assessed on these conventional MRI images. Remyelination can be defined as thin myelin sheets occurring at the edge or throughout a lesion [18]. For monitoring treatment effects it would be beneficial to

monitor remyelination and distinguish it from demyelination and surrounding normal-appearing WM (NAWM). Therefore, several studies have looked at distinguishing demyelination and remyelination with quantitative post-mortem MRI and subsequent histological validation of matched tissue type [18, 19]. These studies showed that some distinctions can be made, especially between remyelination and demyelination, but not between remyelination and NAWM [19]. Although remyelinated tissue has signal intensities in between demyelination and NAWM, the three groups (NAWM, demyelination, and remyelination) have overlapping quantitative MRI values [18]. Within the cycle of Fig. 1, radiological optimization has not been fully successful, indicating limited clinical value for distinguishing and monitoring remyelination. Investigating this method at higher field strengths may yield better results that may subsequently be implemented in the setting of MS *in vivo*.

A study by Yao *et al.* [20] included quantitative MRI at ultra-high field strength (7T and 11.7T), with histology to characterize the pathological features of iron and myelin in WM lesions. They found that while R2\* reduction (inverse transverse relaxation time constant) corresponded to severe loss of both iron and myelin, a negative phase shift (of susceptibility-weighted images) corresponded to focal iron accumulation [20]. This indicates a differential pathological sensitivity of R2\* and negative phase shift (for myelin and iron, respectively). The results of this pathological validation have yet to show its clinical applicability.

### GM Lesions in MS

Cortical GM lesions, in contrast to lesions of the WM, are generally characterized by an intact blood-brain barrier and a lack of inflammatory cell infiltration [21, 22] and relate to physical disability, cognition, and disease progression [23–25]. One of the first post-mortem MRI and histology studies, at 0.6T, showed that cortical lesions as scored on MRI were dramatically under-reported when directly compared to histology of the same brain slice [26]. In subsequent years, with conventional MRI sequences at 1.5T, only up to 5% of histopathologically-defined cortical lesions could be detected [27]. To increase lesion detection rates, new MRI sequences were developed, such as a phase-sensitive inversion recovery or double inversion recovery (DIR) sequence. The latter suppresses the signal of both the CSF and WM, thereby allowing better visualization of the cortex. Nevertheless, even with these newly-developed sequences, ~ 82% of cortical lesions remained undetected by MRI as seen by Seewann and colleagues in a post-mortem MRI with subsequent histology study [28].

An increase in field strength was the next logical step as this can increase the signal-to-noise ratio and spatial

resolution. Initial studies comparing DIR at 1.5T and 3T showed improved cortical lesion detection by 192% with 3T [29]. The pathological specificity of DIR was also tested in a study comparing a DIR and a FLAIR sequence, in which DIR showed its superiority over FLAIR in detecting cortical lesions in MS (Fig. 2) [28]. This led to the publication of consensus recommendations for scoring MS cortical lesions using DIR [30]; these are used in multi-center settings with similar protocols. This is a good example of radiological development of MRI to better reflect histology, and implementation in the clinical setting (Fig. 1).

Although  $\sim 18\%$  visibility with 3T DIR was an increase from the  $\sim 5\%$  with conventional MRI, the question remained if this percentage could be further increased, perhaps by further increasing the field strength. One large post-mortem MRI study compared five sequences (DIR, FLAIR, T2, T2\*, and T1) at two field strengths (3T and 7T). Results from this study showed that only 7T FLAIR and T2\* detected significantly more cortical lesions than 3T FLAIR and T2\* respectively [31]. The sensitivity of 7T MRI was  $\sim 28\%$  when the MRI rater was blinded to histological data. However, when the MRI rater saw the histopathology of the same brain slice, and then looked back at the MRI, the sensitivity rate went up to  $\sim 84\%$  [32]. This effect of increased retrospective sensitivity after knowing the lesion type and location was also found in another study [33]. It has been suggested that continuous observer training (with histological validation) on which signal changes may indicate a lesion, rather than a further increase in field strength, may increase prospective cortical lesion detection [32].

### Post-mortem MRI and Histology in AD

AD, a neurodegenerative disorder characterized by memory disturbances, can only be diagnosed with absolute certainty *via* neuropathological examination of the hallmarks amyloid-beta (A $\beta$ ) plaques and (p-)tau neurofibrillary tangles (NFTs). In both clinical and research settings, diagnosis is generally based on CSF biomarkers, MRI, and clinical symptoms, but unfortunately the accuracy is still unsatisfactory [34]. The AD research field has shown great interest in MRI as a possible biomarker for diagnosis, due to its potential to detect atrophy and pathological hallmarks non-invasively in an *in vivo* setting. Therefore, post-mortem MRI-pathology studies are extremely valuable, as they can verify the histological substrate of the observed contrast by direct comparison.

### Atrophy in AD

Apostolova and colleagues explicitly endorse “the need for pathologic validation of clinical diagnostic criteria and any and all biomarker proposed to be useful for diagnosing AD or tracking its course over time” [35]. Hippocampal atrophy is the most widely-used MRI biomarker for AD to date, differentiating and predicting AD from non-neurological controls [36, 37] as well as AD from mild cognitive impairment [38, 39]. An initial study exploring the pathological validation of hippocampal atrophy found a negative relationship between ante-mortem hippocampal volume and post-mortem Braak and Braak staging [40]. A more recent study scanned hippocampi *ex vivo* at 7T and investigated hippocampal volume in relation to the burden of A $\beta$  and phosphorylated (p-)tau as well as the neuronal count. In addition to a relationship with Braak and Braak staging, they found associations between hippocampal volume and (p-)tau, A $\beta$  burden, and neuronal count. In addition, some regional associations were found; A $\beta$  in the cornu ammonis (CA)1 and subiculum lead to a decrease in global hippocampal volume, as well as (p-)tau in CA2 and CA3, and neuronal count in CA1, CA3, and CA4 [35]. Since within-subfield segmentation of the hippocampus is still challenging (even at 7T) [41], correlations between hippocampal sub-region volume and pathological burden have yet to be undertaken and its clinical relevance to be determined.

### Parenchymal Pathology in AD

Ultra-high field MRI provides sufficient spatial resolution and signal-to-noise ratio needed to image A $\beta$  plaques, but not NFTs. Already in 1999, Benveniste and colleagues found that hypointensities seen on *ex vivo* T2\*-weighted MRI correspond with neuritic plaques [42]. The close relationship between MRI contrast and A $\beta$  plaques was later confirmed in both AD patients and APP/PS1 mice *via* direct comparison of 7T T2\* images and histology, using specifically-designed histological coils [43, 44]. However, further analysis of A $\beta$  plaques suggested that increased iron is responsible for the inherent contrast. Nabuurs and colleagues studied the MRI properties of the different cerebral A $\beta$  plaques, and found that fibrillary A $\beta$  (Congo Red-positive), present in both vascular and parenchymal focal A $\beta$  plaques, but not in diffuse plaques, induces significant changes in the T2\* and T2 signals. Diffuse A $\beta$  remained visually and quantitatively undetected with T2 and T2\* (Fig. 3) [45]. This indicates that both iron and fibrillar A $\beta$  contribute to the hypointense signal on *ex-vivo* MRI. Nevertheless, accurate *in vivo* detection of A $\beta$ -plaques is yet to be achieved.



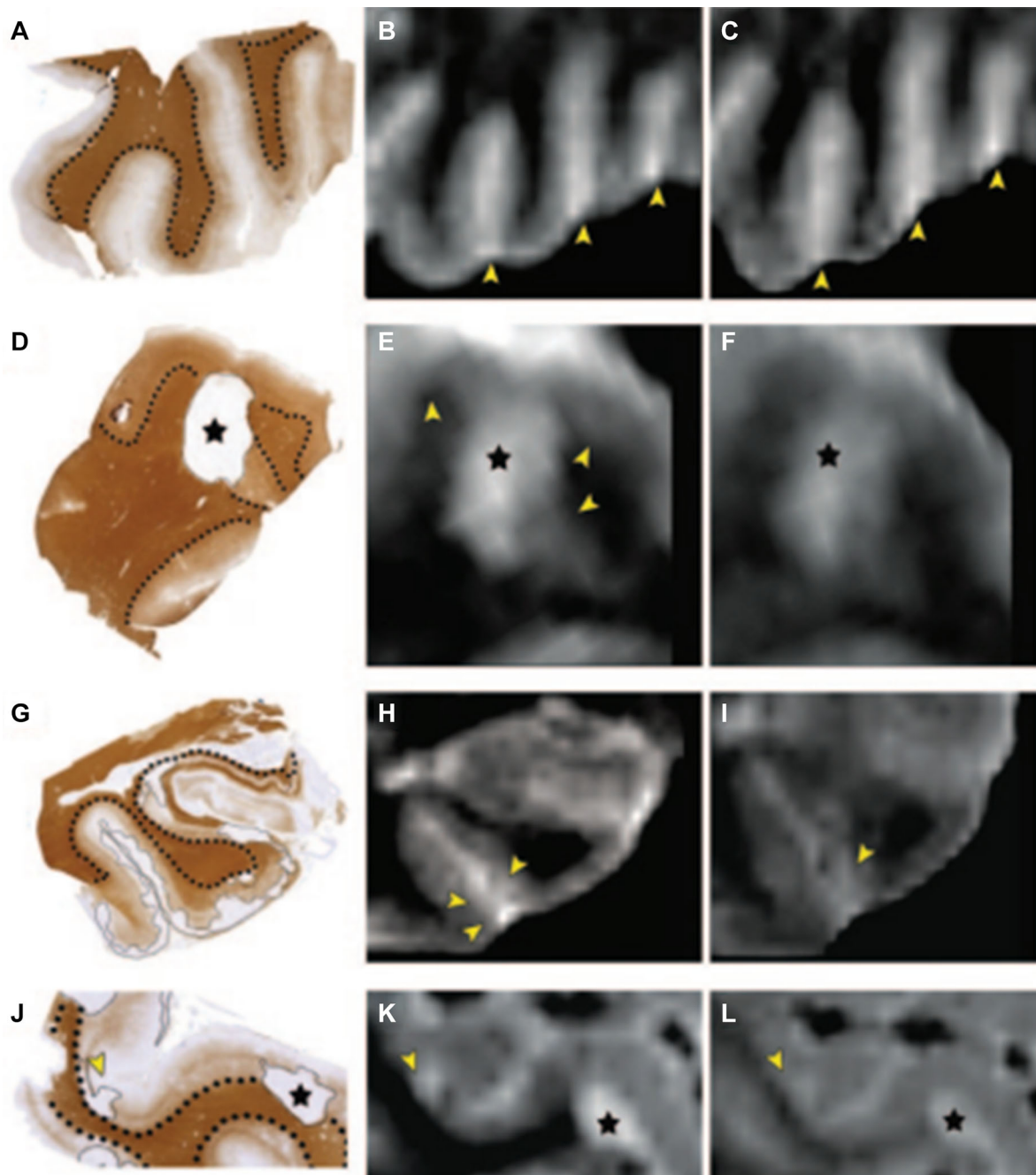


**Fig. 2** Examples of postmortem MRI at 1.5T, with corresponding histopathology. **A, D, G, J** Tissue sections stained for proteolipid protein; dotted lines indicate borders between white and gray matter; cortical lesions are encircled by thin black lines. **B, E, H, K** Postmortem 3D double inversion recovery (DIR) images corresponding to the tissue sections. **C, F, I, L** Corresponding 3D fluid-attenuated inversion recovery (FLAIR) images. **A–C** Multiple sclerosis cortex with rather inhomogeneous signal intensity on MRI, but without any demyelinated lesions. The bright signals indicated by the arrowheads (**B, C**) are caused by blood and other fluid within the sulci, which should not be mistaken for subpial (type III) cortical

pathology. **D–F** Mixed gray-white matter (type I) lesion (asterisk), which is seen on both 3D DIR and 3D FLAIR images. However, the gray matter border (arrowheads in **E**) is often easier to identify on 3D DIR (**E**) than on 3D FLAIR (**F**). **G–I** Subpial (type III) cortical lesions (indicated by thin line in **G** and arrowheads in **H** and **I**) are slightly more conspicuous on 3D DIR (**H**) than on 3D FLAIR (**I**). **J–L** Mixed gray-white matter (type I) lesion (asterisks). Arrowheads in **J–L**: an intracortical lesion, which was prospectively scored on 3D DIR (**K**) and only retrospectively (i.e., with knowledge of histopathology) on 3D FLAIR (**L**). Reprinted from Seewann *et al.* [28] with permission from Wolters Kluwer Health

Aside from the pathological hallmarks of A $\beta$  and NFTs, Zeineh and colleagues investigated the contribution of microglia and iron to signal intensity changes at 7T. Using *ex-vivo* MRI at 0.1 mm isotropic resolution and co-registration with successive histological triple staining for iron, A $\beta$ , and CD163 (a microglial marker), they were able to establish iron accumulation inside activated microglia to be responsible for the MR hypointensities, primarily in the subiculum [46]. Since all cases were late-stage AD, future work is needed to elucidate the role of microglia and iron across the spectrum of non-neurological controls, mild cognitive impairment, and AD.

Using ultra-high field MRI on small tissue samples of the frontal cortex, altered contrast of cortical texture was observed in AD patients. Pixel-wise spatial correlation of signal intensity was calculated based on histology-MRI registration, and showed that the altered contrast could be explained by a combination of increased iron and changes in cortical myelin. Furthermore, this study showed that neuropathological correlates of early- and late-onset AD are distinguishable on 7T T2\* MRI [47]. Nevertheless, its utility for clinical applications needs to be further investigated.

More recent studies have elaborated on this work by investigating changes in cortical texture in whole-brain imaging, and by verifying its relationship with cortical myelo- and cytoarchitecture. Kenkhuis and colleagues characterized the visibility of myelo-architectural changes in AD patients and subsequently investigated the pathological substrate of cortical laminar alterations. Increased variability in visible cortical lamination and severely disturbed cortical lamination was observed in the medial temporal lobe of AD patients. Upon histological inspection of these cases, correspondence with diffuse myelin-associated iron accumulation and A $\beta$ -associated iron deposits was found [48].

### Vascular Pathology in AD

In addition to parenchymal pathology, cerebrovascular disease plays an important role in cognitive decline and dementia. At autopsy, the majority of AD patients exhibit cerebral amyloid angiopathy (CAA) and/or small vessel disease [49], which include lacunar infarcts, white matter hyperintensities (WMHs), microbleeds, and cerebral microinfarcts (CMIs) [50].

CAA is caused by A $\beta$  deposits within predominantly leptomeningeal and intracortical arteries, arterioles, and capillaries [49]. Vascular A $\beta$  deposition has been suggested to cause microvascular lesions including microbleeds and microinfarcts, though definitive evidence remains absent [51–54]. As noted earlier, fibrillary A $\beta$  inside vascular A $\beta$  deposits can cause significant changes in T2\*

and T2 signals [45]. However, when imaging CAA in AD, it is predominantly the harmful microvascular lesions that are imaged, as discussed in the following paragraphs.

WMHs are predominantly of ischemic origin, but non-ischemic demyelinated areas have also been reported [55]. They are easily detectable patches of increased hyperintensity on T2\* MRI and are commonly seen in elderly patients. Literature suggests that such hyperintensities predict AD prior to the clinical stage of the disease [56].

Microbleeds on the other hand have been found to predict mortality, due to their association with increased risk for cardiovascular events and cardiovascular mortality [57]. MRI with correlative histopathology has shown hemosiderin deposits. Therefore, the hypointense contrast on MRI is hypothesized to be due to ferromagnetic iron present after hemosiderin breakdown at the hemorrhagic site [58]. In addition, there is a strong association between MRI-observed microbleeds and microinfarcts, indicating a shared underlying pathophysiological mechanism, suggested to be CAA [59].

Finally, CMIs are considered to be the most widespread vascular component of small vessel disease, occur in 43% of AD patients, and are associated with poorer cognitive performance [60]. Due to their small size, microinfarcts typically go undetected on MRI. However, a study by van Veluw *et al.* confirmed that *ex vivo* T2 7T MRI can detect microinfarcts as hyperintense focal lesions if they are > 0.5 mm. Upon histological analysis, the MRI-detectable microinfarcts appear as pallid focal lesions of cellular death, attributed to ischemia [61]. Consequently, the authors explored the *in vivo* detection of microinfarcts using 7T MRI. Although they were detectable, the resolution was low and only those > 1 mm could be identified on MRI [61]. These results were confirmed in a study by Niwa *et al.* in which only 33% of the histologically-visible microinfarcts were observed on 3T MRI, none of which were < 1 mm [53]. With the knowledge of how and where to look for microinfarcts, this research has subsequently been taken to the *in-vivo* setting. At 3T, some microinfarcts were visualized and associated with cognitive impairment and dementia [62, 63].

In summary, MRI-pathology studies in AD provide insights into the pathogenic components of AD and the role iron plays in the contrast seen on susceptibility-weighted sequences at ultra-high field MRI. In addition, a translation from the post-mortem setting to the *in-vivo* setting has been made in the ability to detect CMIs that are associated with the clinical phenotype of AD, an excellent example of the full circle as visualized in Fig. 1. However, clinical applicability beyond the research setting is still to be evaluated.

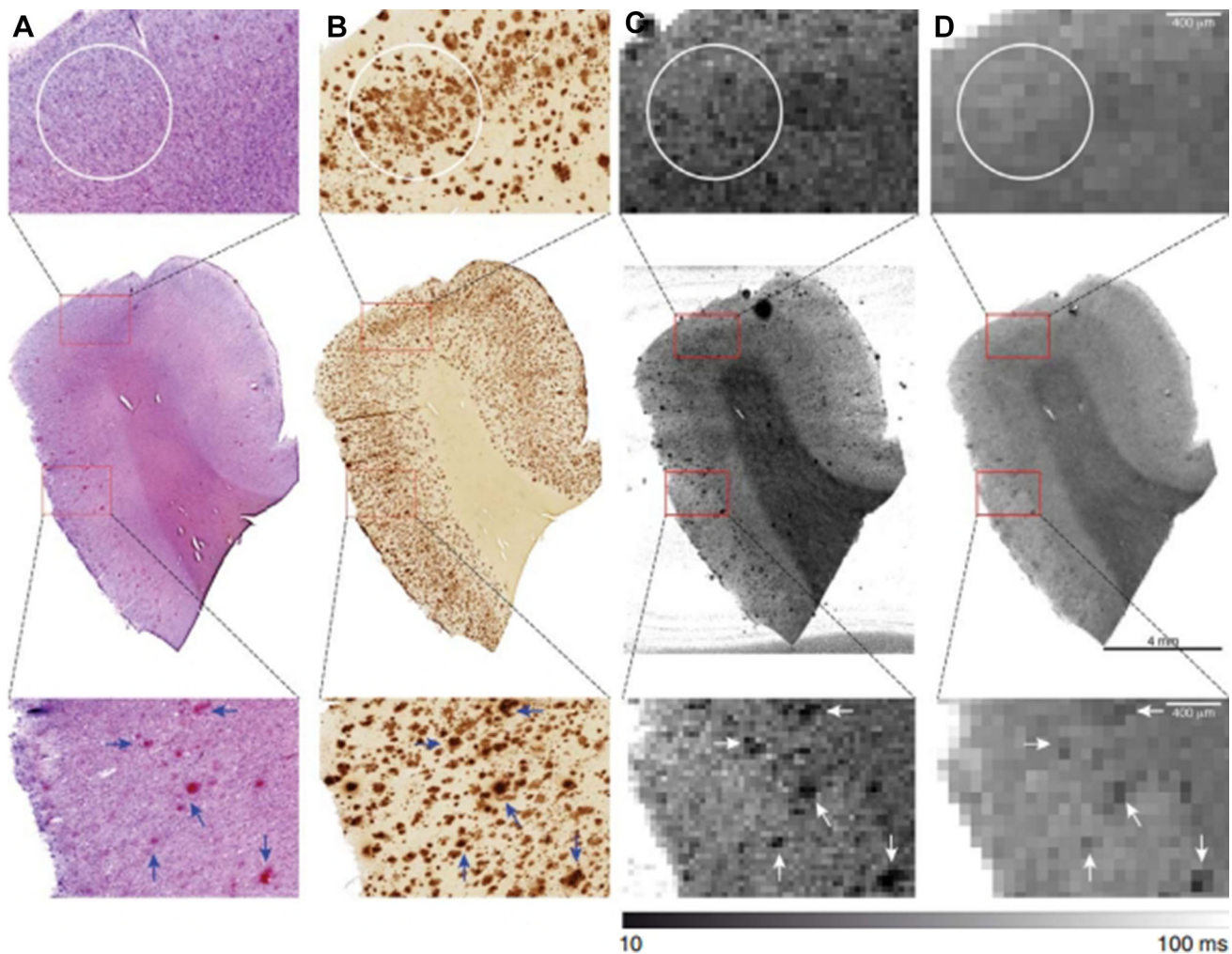


**Fig. 3** Matching of 7T MRI and A $\beta$  histology. Co-registration of (A) Congo Red (CR) and (B) A $\beta$  staining with corresponding quantitative (C) T2\* and (D) T2 maps. No signal decrease was observed corresponding to the outline of areas with A $\beta$  lacking CR positivity (white circles). In contrast, as an example, several but not

all amyloid plaques highlighted by the presence of both CR and A $\beta$  clearly resulted in hypo-intensities on the corresponding MR images (arrows). Reprinted from Nabuurs *et al.* [38] with permission from IOS Press.

### Post-mortem MRI and Histology in PD

PD is a neurodegenerative disorder with neural aggregates containing alpha-synuclein, named Lewy bodies and Lewy neurites, as its pathological hallmark [64]. The subthalamic nucleus (STN), substantia nigra (SN), and locus coeruleus (LC) are nuclei of interest for treating and diagnosing PD and related disorders. Unfortunately, due to their small size, these structures and their subcomponents have been difficult to visualize with conventional MRI sequences at standard field strength. However, with increasing field strength and advanced MRI sequences, increased anatomical accuracy is possible [65]. As such, early detection of SN degeneration or differential diagnosis based on these anatomical locations may now be possible. We discuss these advancements in the following paragraphs.

### Anatomy of the STN

Combined post-mortem imaging and histological studies in PD are still scarce. Most studies have focused on imaging the STN with subsequent histology to evaluate its anatomy [66–68] and utility as a target for deep brain stimulation (DBS) in PD [67, 69, 70]. Initial studies were set up to define MRI-based criteria for electrode placement in DBS, such as correlating T2-weighted hyposignal in the subthalamic region to iron content in the STN [66]. Nevertheless, using conventional MRI sequences such as T2-weighted, the STN is not clearly defined, and this has been confirmed by pathological reports of inaccuracies in electrode placement [71]. However, at 9.4T MRI with subsequent histological validation, the anatomical borders of the



STN are much more clearly defined and significant anatomical variability is apparent [68].

In turn, Al-Helli and colleagues used post-mortem 9.4T MRI and histology to assess the anatomical accuracy of lead placement after MRI-guided, MRI-verified STN DBS [69]. DBS is used in selected patients with PD when a reduced quality of life is the result of insufficient improvement of motor symptoms after medical management alone. The gold standard for verification of the anatomical location of electrodes is post-mortem [72, 73]. Al-Helli and colleagues fixed brain tissue with the electrode still *in situ*, to keep the integrity of the tissue as intact as possible. They only removed the electrodes before MRI scanning, during which they were able to visualize the track and lead placement, in different MRI planes. On T2-weighted 9.4T MRI, the electrode tracks were clearly visible as a hypointense rings, reaching the STN. Subsequently, they used histology to visualize the electrode tracks which showed lymphocytes, gliosis, microglia, and macrophages in the surrounding tissue. They concluded that there is a good correspondence between the two modalities (MRI and histology) and that an MRI-guided, MRI-verified approach for DBS can accurately target the STN [69].

### Imaging the SN

Other studies have focused more on assessing the ability to detect disease-specific changes with MRI, such as visualization of the SN and associated dopaminergic cell loss in this region. A post-mortem MRI and pathology study with conventional T1-weighted imaging at 3T showed that hyperintense areas in the SN pars compacta (SNpc) of a control donor were related to the presence of neuromelanin-containing neurons, while the iso-intense areas in the SNpc in PD and dementia with Lewy bodies were associated with a loss of neuromelanin-containing neurons [74]. Particularly, the nigrosomes, substructures of the SNpc, undergo extensive dopaminergic cell loss. Pathological studies show that cells of nigrosome 1 (N1) are affected in the early stages of PD, sequentially followed by cells in N2, N4, N3, and finally N5 in the later disease stages [75].

Blazejewska and colleagues showed that visualization of N1 within the SNpc is possible with 7T MRI. They scanned the post-mortem midbrains from 2 non-neurological controls and 1 PD patient with T2\* and subsequently stained the brain sections with Perl, a stain for iron and neuromelanin. A hyperintense area within the dorsolateral border of the SNpc was observed in the non-neurological cases. Histopathologically, this was a calbindin-negative region with dopaminergic cells (TH-positive) within a larger calbindin-positive area; the location of N1. Following this,

they scanned 10 PD patients and 8 age-matched healthy controls *in vivo* and found that this previously-identified hyperintense region was bilaterally absent in PD cases, while present in 7 out of 8 controls. They concluded that these post-mortem and *in vivo* changes may provide a tool for detecting and studying the progression of PD [76].

A more recent study also included the other nigrosome subregions of the SN, and used an even higher field strength of 9.4T with histological validation. This study included 10 controls, 5 PD cases, and 8 cases with progressive supranuclear palsy (PSP) [77]. Massey and colleagues were able to identify high-signal structures in controls as nigrosomes and to delineate all five substructures. In addition, they showed that these high-signal structures were still present in PD, indicating that even with dopaminergic cell loss, the distinctive compartmental patterns of nigrosomes are still preserved [77], in accord with the literature on PD pathology [75, 78]. Furthermore, Massey and colleagues found that these high-signal structures were absent in PSP, indicating destruction of the nigrosome compartments [77] and a possible differential biomarker between PD and PSP.

Knowledge gained from these post-mortem MRI and pathology studies on nigrosomes was followed up *in-vivo*, in which researchers tried to visualize all five nigrosomes in 26 PD cases and 15 healthy controls at 7T MRI. Although all nigrosomes (N1–N5) could be identified, N1 was identified with highest confidence in controls and the signal intensity was abnormal (lower) in all PD cases and correlated with the Unified PD Rating Scale, making this the most promising SN biomarker in PD [79].

### Imaging the LC

The LC, through its noradrenergic connections, has been implicated in neurodegenerative disorders [80, 81]. Keren and colleagues visualized the LC at 7T MRI and showed the steps for optimizing MRI sequences (Fig. 4) [82]. Optimization from a sequence used *in vivo* at 3T to *ex-vivo* at 7T is necessary as increasing the field strength lengthens the T1 time and converges longitudinal relaxation, often limiting tissue contrast. In addition, effects of fixation need to be taken into account [83, 84]. The Keren study further showed that MRI contrast in the LC is primarily driven by neuromelanin [82]. Subsequently, Priovoulos and colleagues improved 7T MRI sequences for LC visualization in the clinical research setting [85].

In summary, post-mortem MRI and histology in PD have mainly focused on a few small regions; the STN, SN, and LC. The first as an important endpoint for DBS and the other two as regions associated with dopaminergic and noradrenergic cell loss, for which MRI visualization would be a possible non-invasive biomarker. For both regions,



anatomical accuracy is limited at lower field strengths with conventional sequences, therefore much effort has been made in optimizing the anatomical accuracy with advanced, iron-related sequences at ultra-high field strength, using histology as a gold standard. Some initial steps have already been made in translating these findings back to the clinical research setting [79, 85]. Future studies will have to show the utility of these accurate anatomical maps and signal changes in defining and monitoring disease progression in PD.

## TBI and Stroke

A limited number of post-mortem MRI studies have been performed on cases of TBI and stroke. One of the main reasons is that *in vivo* MRI is rarely performed in the acute stages of TBI due to time constraints and difficulties in actively monitoring the patient within a magnetic field [86]. For this reason, computed tomography (CT) is more commonly used. Nevertheless, there is convincing evidence that MRI is more sensitive than CT for TBI [87, 88], including an initial study by Jones and colleagues who directly compared MRI, CT, and neuropathology. Six patients with severe TBI had ante-mortem CT and post-mortem 1.0T MRI with neuropathological assessment. Their results showed that MRI detected ~ 23% of pathological lesions, while CT only detected ~ 5%, a difference that was more prominent in smaller lesions. In addition, CT underestimated the lesion size by ~ 50%, while T2 images more closely approximated the pathological size than T1 images [86]. In stroke, a systematic review and meta-analysis in animals (rats, mice, and baboons) also found that T2 imaging is most effective for estimating infarct size, based on histological comparison [89].

In the study by Jones *et al.*, non-hemorrhagic lesions of diffuse axonal injury were not detected by CT or by conventional low field-strength MRI sequences. More recent studies at higher field strength that also include hemorrhagic lesions, have looked at apparent diffusion coefficient (ADC) maps for depicting brain ischemia, and found a 73%–92% sensitivity in the first 3 h and 95%–100% in the first 6 h [88]. In a rat model, the spatiotemporal progression of the ADC of water was further investigated, showing an early decrease (when CT and T2 are still normal), then ‘pseudo-normalization’, with a subsequent increase due to cell lysis and necrosis [88, 90]. Nevertheless, human post-mortem MRI validation studies are still lacking, but could be valuable to better understand the influence of stroke on surrounding tissue and how this may be reflected on MRI.

Repetitive TBI may lead to a progressive degenerative disorder termed chronic traumatic encephalopathy (CTE). Pathological findings in CTE consist of the accumulation of hyperphosphorylated tau, myelin loss, axonal injury, and WM degeneration [91]. Holleran and colleagues tested the hypothesis that diffusion MRI might be useful for detecting WM microstructural changes in areas near tau pathology. They scanned formalin-fixed tissue blocks from pathologically-defined CTE patients with 11.4T MRI and subsequently performed histological assessment for (p-)tau and axonal disruption. Their results showed that fractional anisotropy was associated with WM axonal damage, which was more pronounced in regions with adjacent GM (p-)tau pathology. They concluded that *ex vivo* diffusion MRI is sensitive for the microstructural changes in CTE, but that application in the *in vivo* setting has yet to be determined [91]. Nevertheless, initial *in vivo* studies show promising results [92].

## Summary, Discussion, and Future Prospects

This review provides an overview of studies combining post-mortem MRI and histology in MS, AD, and PD, not only to better visualize the anatomy and pathology, but also to understand how this knowledge can be applied in the clinical setting.

In MS, the main aims are to be able to differentiate demyelinating lesions from areas of remyelination, and improve the visualization of GM lesions. Pathological distinction of WM lesion types with quantitative MRI has many overlapping values, hence limiting clinical applicability [18, 19]. Future studies at high or ultra-high field strength may provide better differentiation with more clinical utility. Regarding the visualization of GM lesions, retrospective inspection (with histopathological knowledge of lesion type and location) visualizes up to ~ 80% of lesions, in contrast to the ~ 30% at prospective inspection [32]. Therefore, research suggests that training sessions with histological validation can decrease this discrepancy in future studies and perhaps in clinical practice [32].

In AD, initial studies focused on the visualization of A $\beta$  pathology (through T2\* signal changes) with smaller tissue samples at increasing field strengths [42, 45]. The possible clinical and research applicability of these signal changes only became apparent in later years, when post-mortem differentiation between early and late onset AD could be made [47]. An excellent example of successful translation from post-mortem MRI to the clinical research setting is the visualization of CMIs; their detection as hyperintense focal lesions on *ex vivo* 7T MRI with histopathological validation [61], then on *in vivo* 7T MRI in the same study [61], and subsequently on *in vivo* 3T MRI [62, 63], which

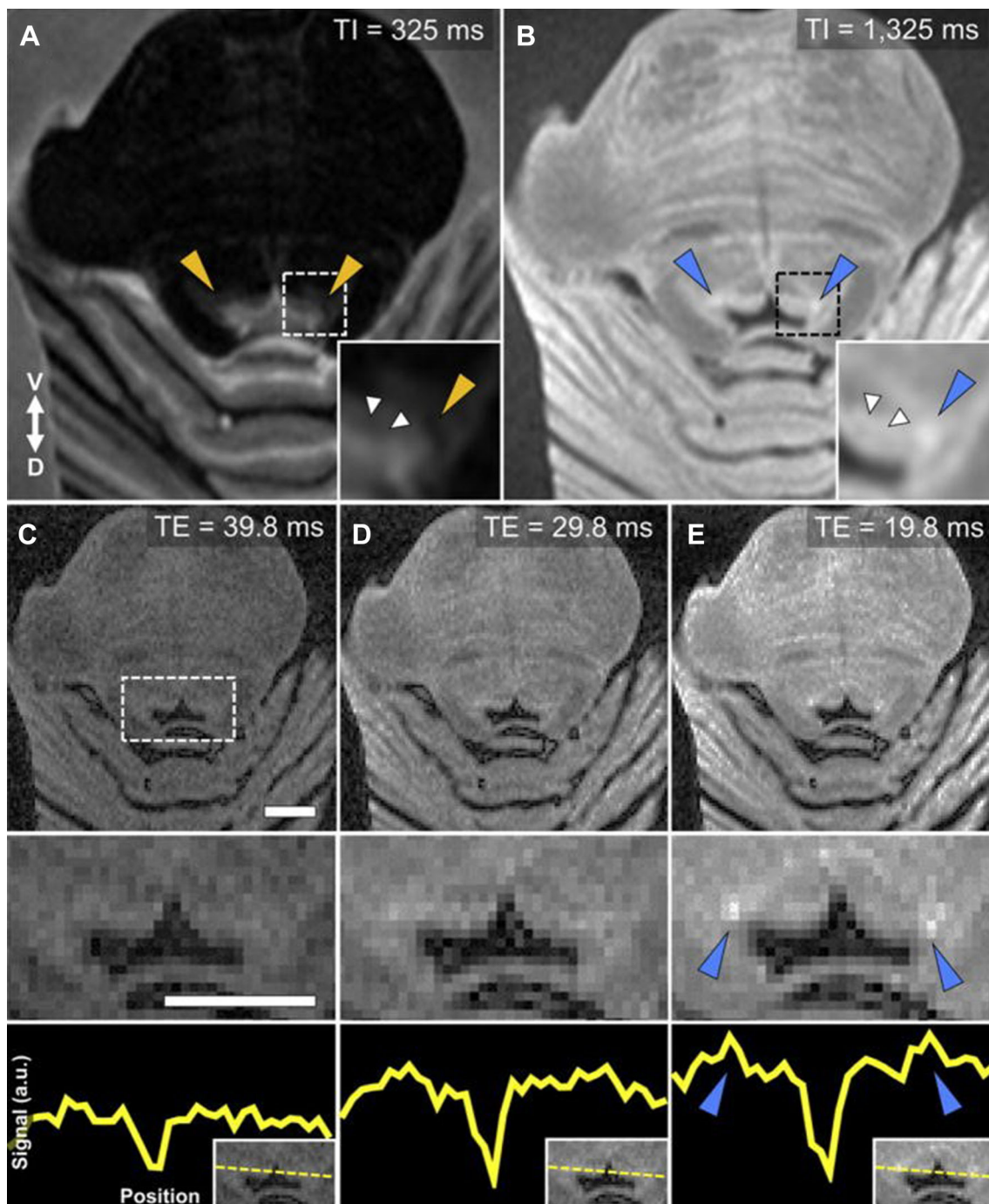


**Fig. 4** Optimal parameters for *ex-vivo* LC-MRI. A rapid acquisition with a refocused echoes (RARE) sequence was used to obtain axial sections from brainstem tissue embedded in agar. **A** A short inversion recovery time (TI) produces distinct periaqueductal gray (PAG) contrast compared to surrounding tissue, but no elevated contrast in putative LC regions (orange triangles). **B** Elevated contrast is still seen in the PAG with a long TI, as well as specific increased contrast in putative LC regions (blue triangles). **C–E** A short echo time (TE) results in diminished PAG contrast relative to increased contrast in the LC (blue triangles). Magnified 4th ventricular area (dashed box) is presented in the middle row. The bottom row shows the relative increase in LC-MRI contrast with shorter TE using a linear ROI that

was used to collect contrast values across the brainstem for each TE acquisition (y-axis: arbitrary units). An axial slice from the same tissue sample (HB 24) is presented in all images (ROI positioning shown in the inset at bottom right). Image parameters common across scans: number of slices = 8, slice thickness = 2 mm, slice spacing = 0.5 mm, repetition time = 3000 ms, inversion time = 825 ms, number of averages = 3, imaging resonance frequency = 300 MHz, echo train length = 2, flip angle = 180°, matrix size = 128 × 128, field of view = 4.00 × 4.00 cm, in-plane voxel size = 310 μm. Scale bars, 5 mm. Reprinted from Keren *et al.* [69] with permission from Elsevier.

could be related to the clinical phenotype (cognitive impairment) [62, 63].

In PD, post-mortem imaging studies mainly involve obtaining better anatomical visualization of the STN, SN, and LC. The clinical value is directly apparent for the STN, as better visualization of its borders is paramount for effective DBS [68, 69]. For the SN and LC, post-mortem MRI and histological studies are making the first strides towards using these locations as MRI biomarkers in differentiating diseases (PD or PSP) [77] or disease stages (sequential degeneration of nigrosomes) [75, 77]. Nevertheless, replication in larger *in vivo* cohorts is required to better assess its value in clinical implementation.

In TBI, studies combining post-mortem MRI and histology are still few, which may be due to the preference of CT over MRI in the clinical setting, as severely injured patients cannot be actively monitored in the proximity of a strong magnet. Nevertheless, the available post-mortem MRI and histology studies show that MRI is more sensitive to lesion size than CT [86] and diffusion MRI is sensitive to subtle microstructural changes, such as axonal disruption [91]. These are promising results which may have clinical value for patients not in the acute phase of TBI, such as monitoring recovery.

The above paragraphs show that for both MS GM lesions and AD-related microinfarcts, not necessarily developing or optimizing MRI sequences, but training of MRI users is more important for clinical implementation (Fig. 1). Microinfarcts are very likely to be visible on *in vivo* 3T MRI, but it is difficult to find them if you do not know where to look. Knowing where to look, by examining ultra-high field MRI with histological validation, is teaching researchers, and perhaps in future also radiologists, to better gauge where to look at clinical resolution and field strength MRI. Perhaps PD research, which often focuses on small brainstem nuclei, could benefit from this knowledge in translating post-mortem MRI findings to clinical practice.

While MS and AD studies focused on visualizing pathology in specific cortical regions, PD studies were initially left behind due to the difficulty in visualizing the small anatomical structures in the brainstem. By increasing the field strength and using more advanced MRI sequences, increased anatomical accuracy became possible. The use of a reliable anatomical atlas is crucial for subsequent clinical investigation. Therefore, the combination of post-mortem MRI and histology has played an important role in creating and validating several cortical and subcortical atlases [70, 93, 94] and software packages [95]. Some are based on a single brain [93, 94], and others on several brain specimens [96]. A recent development not only includes histology and multimodal MRI, but also structural connectivity using tractography-based parcellation [70]. This

approach is especially interesting in defining DBS targets and assessing their projections.

The studies described in this review show various MRI sensitivities for a variety of pathological hallmarks such as demyelination, dopaminergic cell loss, and deposits of fibrillary A $\beta$ . Nevertheless, while these images can visualize the presence or absence of pathology, they are not very pathologically specific; T2\* imaging appears to be the optimal sequence for all of these hallmarks. However, with the considerable clinical heterogeneity in neurodegenerative diseases and substantial discrepancies between clinical diagnoses relative to pathology [34, 97, 98], it is not only imperative to be pathologically sensitive, but also pathologically specific.

Currently, conventional imaging techniques (e.g. T1-weighted or T2-weighted MRI) are too insensitive to pick up on disease-specific subtleties; many cortical lesions are still missed in MS, and in AD and PD generally no cortical changes are observed with conventional MRI. Therefore, these studies may benefit from a more quantitative MRI approach, such as relaxometry, quantitative susceptibility mapping (QSM), and diffusion tensor or magnetization transfer imaging combined with pathology, as these quantitative measures may be more pathologically specific. In regards to the quantification of iron deposition *in vivo*, QSM has become the preferred approach [99], but has yet to be verified post-mortem. In addition, these quantitative MRI techniques can be used exploratively towards deep learning techniques to pick up subtleties even better than the human eye [100, 101].

Nevertheless, even post-mortem MRI and pathology studies have their limitations. Both post-mortem delay and formalin fixation have effects on MRI relaxometry [83, 84], therefore direct comparison between the post-mortem and *in vivo* settings is generally not possible. Nevertheless, when using quantitative MRI, relative comparison seems feasible; the magnetization transfer ratio of cortical MS lesions compared to surrounding normal-appearing gray matter is lower both post-mortem and *in vivo* [102, 103], and dichotomous signal intensities (hyper- or hypointense) do not seem to change between the post-mortem and *in vivo* settings [61, 63, 76]. In addition, although comparison of ante-mortem and post-mortem MRI in humans is lacking, a study in rodents showed no significant changes in the volumetric measurements of anatomical structures [104].

A post-mortem study in forensic medicine furthermore shows that not only post-mortem delay, but also the cause of death has a differential impact on diffusion measures; ADC are significantly lower in mechanical and hypoxic brain injury than in brains from patients who died from heart failure [105], something that researchers should take into account when studying donors with different causes of



death. Although it is not possible to follow signal changes due to pathological changes over time in longitudinal MRI-pathology studies, it may be feasible to obtain donors at different stages of disease [106], or use an *in-vivo* derivative of pathology such as A $\beta$  positron-emission tomography imaging, previously validated with post-mortem MRI and histology [107]. Furthermore, the availability of samples for post-mortem MRI and histology may be limited, sometimes due to the low prevalence of a disease. In such cases, collaboration with multiple international brain banks may aid researchers, although uniformity in tissue collection is required.

This review has shown various ways in which post-mortem MRI and pathology have supported clinical research, not only by validating sequences, but also by coming up with suggestions for clinical implementation. Some have been quite successful [30, 61], while others require further validation before implementation [76]. In conclusion, there is much to gain from post-mortem MRI and pathology studies, which should be further explored as new clinical questions emerge.

**Conflict of interest** L. E. Jonkman is financially supported by a grant from the Alzheimer's Association (AARF-18-566459). B. Kenkhuis has no conflict of interest. J. J. G. Geurts is an editor of MS Journal. He serves on the editorial boards of Neurology and Frontiers of Neurology and is President of the Netherlands Organization for Health Research and Innovation. He has served as a consultant for Merck-Serono, Biogen, Novartis, Genzyme, and Teva Pharmaceuticals. W. D. J. van de Berg is financially supported by grants from Amsterdam Neuroscience, ZonMW Memorabel, ZonMW Technology Hotel, Stichting Parkinson Fonds, Alzheimer Netherlands-LECMa, Roche Pharma, Lysosomal Therapeutics, and Cross-beta Sciences. She is a consultant for CHDR Leiden and Lysosomal Therapeutics.

## References

1. Josephs KA, Dickson DW, Tosakulwong N, Weigand SD, Murray ME, Petrucelli L, *et al.* Rates of hippocampal atrophy and presence of post-mortem TDP-43 in patients with Alzheimer's disease: a longitudinal retrospective study. *Lancet Neurol* 2017 16: 917–924.
2. Kantarci K, Murray ME, Schwarz CG, Reid RI, Przybelski SA, Lesnick T, *et al.* White-matter integrity on DTI and the pathologic staging of Alzheimer's disease. *Neurobiol Aging* 2017, 56: 172–179.
3. Nedelska Z, Ferman TJ, Boeve BF, Przybelski SA, Lesnick TG, Murray ME, *et al.* Pattern of brain atrophy rates in autopsy-confirmed dementia with Lewy bodies. *Neurobiol Aging* 2015, 36: 452–461.
4. Raman MR, Preboske GM, Przybelski SA, Gunter JL, Senjem ML, Vemuri P, *et al.* Antemortem MRI findings associated with microinfarcts at autopsy. *Neurology* 2014, 82: 1951–1958.
5. Petzold A, Tozer DJ, Schmierer K. Axonal damage in the making: neurofilament phosphorylation, proton mobility and magnetisation transfer in multiple sclerosis normal appearing white matter. *Exp Neurol* 2011, 232: 234–349.
6. Seehaus AK, Roebroek A, Chiry O, Kim DS, Ronen I, Bratzke H, *et al.* Histological validation of DW-MRI tractography in human postmortem tissue. *Cereb Cortex* 2013, 23: 442–450.
7. Hametner S, Endmayr V, Deistung A, Palmrich P, Prihoda M, Haimburger E, *et al.* The influence of brain iron and myelin on magnetic susceptibility and effective transverse relaxation: a biochemical and histological validation study. *Neuroimage* 2018, 179: 117–133.
8. Meijer FJA, Goraj B. Brain MRI in Parkinson's disease. *Front Biosci (Elite Ed)* 2014, 6: 360–369.
9. Bell JE, Alafuzoff I, Al-Sarraj S, Arzberger T, Bogdanovic N, Budka H, *et al.* Management of a twenty-first century brain bank: experience in the BrainNet Europe consortium. *Acta Neuropathol* 2008, 115: 497–507.
10. Samarasekera N, Salman RAS, Huitinga I, Klioueva N, McLean CA, Kretschmar H, *et al.* Brain banking for neurological disorders. *Lancet Neurol* 2013, 12: 1096–1105.
11. Beach TG, Adler CH, Sue LI, Serrano G, Shill HA, Walker DG, *et al.* Arizona study of aging and neurodegenerative disorders and brain and body donation program. *Neuropathology* 2015, 35: 354–389.
12. Jonkman LE, Geurts JGG. Postmortem magnetic resonance imaging. *Handb Clin Neurol* 2018, 150: 335–354. <https://doi.org/10.1016/B978-0-444-63639-3.00023-2>
13. Seewann A, Kooi EJ, Roosendaal SD, Barkhof F, van der Valk P, Geurts JGG. Translating pathology in multiple sclerosis: the combination of postmortem imaging, histopathology and clinical findings. *Acta Neurol Scand* 2009, 119: 349–355.
14. Lassmann H. Recent neuropathological findings in MS-implications for diagnosis and therapy. *J Neurol* 2004, 251 Suppl: IV2–IV5.
15. Lucchinetti C, Brück W, Noseworthy J. Multiple sclerosis: recent developments in neuropathology, pathogenesis, magnetic resonance imaging studies and treatment. *Curr Opin Neurol* 2001, 14: 259–269.
16. Matthews PM, Arnold DL. Magnetic resonance imaging of multiple sclerosis: new insights linking pathology to clinical evolution. *Curr Opin Neurol* 2001, 14: 279–287.
17. Miller DH, Grossman RI, Reingold SC, McFarland HF. The role of magnetic resonance techniques in understanding and managing multiple sclerosis. *Brain* 1998, 121: 3–24.
18. Barkhof F, Bruck W, De Groot CJA, Bergers E, Hulshof S, Geurts J, *et al.* Remyelinated lesions in multiple sclerosis: magnetic resonance image appearance. *Arch Neurol* 2003, 60: 1073–1081.
19. Zhang Y, Jonkman L, Klauser A, Barkhof F, Yong VW, Metz LM, *et al.* Multi-scale MRI spectrum detects differences in myelin integrity between MS lesion types. *Mult Scler* 2016, 22: 1569–1577.
20. Yao B, Bagnato F, Matsuura E, Merkle H, Gelderen P van, Cantor FK, *et al.* Chronic multiple sclerosis lesions: characterization with high-field-strength MR imaging. *Radiology* 2012, 262: 206–215.
21. Wegner C, Esiri MM, Chance SA, Palace J, Matthews PM. Neocortical neuronal, synaptic, and glial loss in multiple sclerosis. *Neurology* 2006, 67: 960–967.
22. Peterson JW, Bö L, Mörk S, Chang A, Trapp BD. Transected neurites, apoptotic neurons, and reduced inflammation in cortical multiple sclerosis lesions. *Ann Neurol* 2001, 50: 389–400.
23. Calabrese M, Rinaldi F, Seppi D, Favaretto A, Squarcina L, Mattisi I, *et al.* Cortical diffusion-tensor imaging abnormalities in multiple sclerosis: a 3-year longitudinal study. *Radiology* 2011, 261: 891–898.
24. Roosendaal SD, Moraal B, Vrenken H, Castelijns JA, Pouwels PJW, Barkhof F, *et al.* *In vivo* MR imaging of hippocampal



- lesions in multiple sclerosis. *J Magn Reson Imaging* 2008, 27: 726–731.
25. Roosendaal SD, Moraal B, Pouwels PJW, Vrenken H, Castelijns JA, Barkhof F, *et al.* Accumulation of cortical lesions in MS: relation with cognitive impairment. *Mult Scler* 2009, 15: 708–714.
  26. Kidd D, Barkhof F, McConnell R, Algra PR, Allen IV, Revesz T. Cortical lesions in multiple sclerosis. *Brain* 1999, 122: 17–26.
  27. Geurts JGG, Bö L, Pouwels PJW, Castelijns JA, Polman CH, Barkhof F. Cortical lesions in multiple sclerosis: combined postmortem MR imaging and histopathology. *AJNR Am J Neuroradiol* 2005, 26: 572–527.
  28. Seewann A, Kooi EJ, Roosendaal SD, Pouwels PJW, Wattjes MP, van der Valk P, *et al.* Postmortem verification of MS cortical lesion detection with 3D DIR. *Neurology* 2012, 78: 302–308.
  29. Simon B, Schmidt S, Lukas C, Gieseke J, Träber F, Knol DL, *et al.* Improved *in vivo* detection of cortical lesions in multiple sclerosis using double inversion recovery MR imaging at 3 Tesla. *Eur Radiol* 2010, 20: 1675–1683.
  30. Geurts JGG, Roosendaal SD, Calabrese M, Ciccarelli O, Agosta F, Chard DT, *et al.* Consensus recommendations for MS cortical lesion scoring using double inversion recovery MRI. *Neurology* 2011, 76: 418–424.
  31. Kilsdonk ID, Jonkman LE, Klaver R, van Veluw SJ, Zwanenburg JJM, Kuijjer JPA, *et al.* Increased cortical grey matter lesion detection in multiple sclerosis with 7 T MRI: a post-mortem verification study. *Brain* 2016, 139: 1472–1481.
  32. Jonkman LE, Klaver R, Fleysher L, Inglese M, Geurts JGG. Ultra-high-field MRI visualization of cortical multiple sclerosis lesions with T2 and T2\*: a postmortem MRI and histopathology study. *AJNR Am J Neuroradiol* 2015, 36: 2062–2067.
  33. Pitt D, Boster A, Pei W, Wohleb E, Jasne A, Zachariah CR, *et al.* Imaging cortical lesions in multiple sclerosis with ultra-high-field magnetic resonance imaging. *Arch Neurol* 2010, 67: 812–818.
  34. Beach TG, Monsell SE, Phillips LE, Kukull W. Accuracy of the clinical diagnosis of Alzheimer disease at national institute on aging Alzheimer disease centers, 2005–2010. *J Neuropathol Exp Neurol* 2012, 71: 266–273.
  35. Apostolova LG, Zarow C, Biado K, Hurtz S, Boccardi M, Somme J, *et al.* Relationship between hippocampal atrophy and neuropathology markers: a 7T MRI validation study of the EADC-ADNI harmonized hippocampal segmentation protocol. *Alzheimer's Dement* 2015, 11: 139–150.
  36. Apostolova LG, Mosconi L, Thompson PM, Green AE, Hwang KS, Ramirez A, *et al.* Subregional hippocampal atrophy predicts Alzheimer's dementia in the cognitively normal. *Neurobiol Aging* 2010, 31: 1077–1088.
  37. De Leon MJ, George AE, Golomb J, Tarshish C, Convit A, Kluger A, *et al.* Frequency of hippocampal formation atrophy in normal aging and Alzheimer's disease. *Neurobiol Aging* 1997, 18: 1–11.
  38. Apostolova LG, Dinov ID, Dutton RA, Hayashi KM, Toga AW, Cummings JL, *et al.* 3D comparison of hippocampal atrophy in amnesic mild cognitive impairment and Alzheimer's disease. *Brain* 2006, 129: 2867–2873.
  39. Apostolova LG, Dutton RA, Dinov ID, Hayashi KM, Toga AW, Cummings JL, *et al.* Conversion of mild cognitive impairment to Alzheimer disease predicted by hippocampal atrophy maps. *Arch Neurol* 2006, 63: 693.
  40. Jack CR, Dickson DW, Parisi JE, Xu YC, Cha RH, O'Brien PC, *et al.* Antemortem MRI findings correlate with hippocampal neuropathology in typical aging and dementia. *Neurology* 2002, 58: 750–757.
  41. Giuliano A, Donatelli G, Cosottini M, Tosetti M, Retico A, Fantacci ME. Hippocampal subfields at ultra high field MRI: an overview of segmentation and measurement methods. *Hippocampus* 2017, 27: 481–494.
  42. Benveniste H, Einstein G, Kim KR, Hulette C, Johnson GA. Detection of neuritic plaques in Alzheimer's disease by magnetic resonance microscopy. *Proc Natl Acad Sci U S A* 1999, 96: 14079–14084.
  43. Meadowcroft MD, Connor JR, Smith MB, Yang QX. MRI and histological analysis of beta-amyloid plaques in both human Alzheimer's disease and APP/PS1 transgenic mice. *J Magn Reson Imaging* 2009, 29: 997–1007.
  44. Nabuurs RJA, Hegeman I, Natté R, van Duinen SG, van Buchem MA, van der Weerd L, *et al.* High-field MRI of single histological slices using an inductively coupled, self-resonant microcoil: application to *ex vivo* samples of patients with Alzheimer's disease. *NMR Biomed* 2011, 24: 351–357.
  45. Nabuurs RJA, Natté R, de Ronde FM, Hegeman-Kleinn I, Dijkstra J, van Duinen SG, *et al.* MR microscopy of human Amyloid- $\beta$  deposits: characterization of parenchymal amyloid, diffuse plaques, and vascular amyloid. *J Alzheimer's Dis* 2013, 34: 1037–1049.
  46. Zeineh MM, Chen Y, Kitzler HH, Hammond R, Vogel H, Rutt BK. Activated iron-containing microglia in the human hippocampus identified by magnetic resonance imaging in Alzheimer disease. *Neurobiol Aging* 2015, 36: 2483–2500.
  47. Bulk M, Abdelmoula WM, Nabuurs RJA, van der Graaf LM, Mulders CWH, Mulder AA, *et al.* Postmortem MRI and histology demonstrate differential iron accumulation and cortical myelin organization in early- and late-onset Alzheimer's disease. *Neurobiol Aging* 2018, 62: 231–242.
  48. Kenkhuis B, Jonkman LE, Bulk M, Buijs M, Boon BDC, Bouwman FH, *et al.* 7T MRI allows detection of disturbed cortical lamination in medial temporal lobe in patients with Alzheimer's disease. *Neuroimage Clin* 2019. <https://doi.org/10.1016/j.nicl.2019.101665>.
  49. Attems J, Jellinger KA. The overlap between vascular disease and Alzheimer's disease—lessons from pathology. *BMC Med* 2014, 12: 206.
  50. Pantoni L. Cerebral small vessel disease: from pathogenesis and clinical characteristics to therapeutic challenges. *Lancet Neurol* 2010, 9: 689–701.
  51. Kövari E, Herrmann FR, Hof PR, Bouras C. The relationship between cerebral amyloid angiopathy and cortical microinfarcts in brain ageing and Alzheimer's disease. *Neuropathol Appl Neurobiol* 2013, 39: 498–509.
  52. Soontornniyomkij V, Lynch MD, Mermash S, Pomakian J, Badkoohehi H, Clare R, *et al.* Cerebral microinfarcts associated with severe cerebral  $\beta$ -amyloid angiopathy. *Brain Pathol* 2010, 20: 459–467.
  53. Niwa A, Ii Y, Shindo A, Matsuo K, Ishikawa H, Taniguchi A, *et al.* Comparative analysis of cortical microinfarcts and microbleeds using 3.0-Tesla postmortem magnetic resonance images and histopathology. *J Alzheimer's Dis* 2017, 59: 951–959.
  54. De Reuck JL, Deramecourt V, Auger F, Durieux N, Cordonnier C, Devos D, *et al.* The significance of cortical cerebellar microbleeds and microinfarcts in neurodegenerative and cerebrovascular diseases. *Cerebrovasc Dis* 2015, 39: 138–143.
  55. Fazekas F, Kleinert R, Offenbacher H, Schmidt R, Kleinert G, Payer F, *et al.* Pathologic correlates of incidental MRI white matter signal hyperintensities. *Neurology* 1993, 43: 1683–1689.
  56. Mortamais M, Artero S, Ritchie K. White matter hyperintensities as early and independent predictors of Alzheimer's disease risk. *J Alzheimer's Dis* 2014, 42: S393–S400.

57. Benedictus MR, Prins ND, Goos JDC, Scheltens P, Barkhof F, van der Flier WM. Microbleeds, mortality, and stroke in Alzheimer Disease. *JAMA Neurol* 2015, 72: 539.
58. Fazekas F, Klei­nert R, Roob G, Klei­nert G, Kapeller P, Schmidt R, *et al.* Histopathologic analysis of foci of signal loss on gradient-echo T2\*-weighted MR images in patients with spontaneous intracerebral hemorrhage: evidence of microangiopathy-related microbleeds. *AJNR Am J Neuroradiol* 1999, 20: 637–642.
59. Lauer A, van Veluw SJ, William CM, Charidimou A, Roongpiboonsopit D, Vashkevich A, *et al.* Microbleeds on MRI are associated with microinfarcts on autopsy in cerebral amyloid angiopathy. *Neurology* 2016, 87: 1488–1492.
60. Brundel M, de Bresser J, van Dillen JJ, Kappelle LJ, Biessels GJ. Cerebral microinfarcts: a systematic review of neuropathological studies. *J Cereb Blood Flow Metab* 2012, 32: 425–436.
61. van Veluw SJ, Zwanenburg JJ, Engelen-Lee J, Spliet WG, Hendrikse J, Luijten PR, *et al.* *In vivo* detection of cerebral cortical microinfarcts with high-resolution 7T MRI. *J Cereb Blood Flow Metab* 2013, 33: 322–329.
62. Hilal S, Sikking E, Shaik MA, Chan QL, van Veluw SJ, Vrooman H, *et al.* Cortical cerebral microinfarcts on 3T MRI. *Neurology* 2016, 87: 1583–1590.
63. Ferro DA, van Veluw SJ, Koek HL, Exalto LG, Biessels GJ, Utrecht Vascular Cognitive Impairment (VCI) study group. Cortical cerebral microinfarcts on 3 Tesla MRI in patients with vascular cognitive impairment. *J Alzheimer's Dis* 2017, 60: 1443–1450.
64. Braak H, Del Tredici K, Rüb U, de Vos RAI, Jansen Steur ENH, Braak E. Staging of brain pathology related to sporadic Parkinson's disease. *Neurobiol Aging* 24: 197–211.
65. Massey LA, Yousry TA. Anatomy of the substantia nigra and subthalamic nucleus on MR imaging. *Neuroimaging Clin N Am* 2010, 20: 7–27.
66. Dormont D, Ricciardi KG, Tandé D, Parain K, Menuel C, Galanaud D, *et al.* Is the subthalamic nucleus hypointense on T2-weighted images? A correlation study using MR imaging and stereotactic atlas data. *AJNR Am J Neuroradiol* 2004, 5: 1516–1523.
67. Rijkers K, Temel Y, Visser-Vandewalle V, Vanormelingen L, Vandersteen M, Adriaensens P, *et al.* The microanatomical environment of the subthalamic nucleus. *J Neurosurg* 2007, 107: 198–201.
68. Massey LA, Miranda MA, Zrinzo L, Al-Helli O, Parkes HG, Thornton JS, *et al.* High resolution MR anatomy of the subthalamic nucleus: imaging at 9.4T with histological validation. *Neuroimage* 2012, 59: 2035–2044.
69. Al-Helli O, Thomas DL, Massey L, Foltynie T, Limousin P, Holton JL, *et al.* Deep brain stimulation of the subthalamic nucleus: histological verification and 9.4-T MRI correlation. *Acta Neurochir (Wien)* 2015, 157: 2143–2147.
70. Ewert S, Plettig P, Li N, Chakravarty MM, Collins DL, Herrington TM, *et al.* Toward defining deep brain stimulation targets in MNI space: a subcortical atlas based on multimodal MRI, histology and structural connectivity. *Neuroimage* 2018, 170: 271–282.
71. McClelland S, Vonsattel JP, Garcia RE, Amaya MD, Winfield LM, Pullman SL, *et al.* Relationship of clinical efficacy to postmortem-determined anatomic subthalamic stimulation in Parkinson syndrome. *Clin Neuropathol* 2007, 26: 267–275.
72. Vedam-Mai V, Yachnis A, Ullman M, Javedan SP, Okun MS. Postmortem observation of collagenous lead tip region fibrosis as a rare complication of DBS. *Mov Disord* 2012, 27: 565–569.
73. Sun DA, Yu H, Spooner J, Tatsas AD, Davis T, Abel TW, *et al.* Postmortem analysis following 71 months of deep brain stimulation of the subthalamic nucleus for Parkinson disease. *J Neurosurg* 2008, 109: 325–329.
74. Kitao S, Matsusue E, Fujii S, Miyoshi F, Kaminou T, Kato S, *et al.* Correlation between pathology and neuromelanin MR imaging in Parkinson's disease and dementia with Lewy bodies. *Neuroradiology* 2013, 55: 947–953.
75. Damier P, Hirsch EC, Agid Y, Graybiel AM. The substantia nigra of the human brain. II. Patterns of loss of dopamine-containing neurons in Parkinson's disease. *Brain* 1999, 122 (Pt 8):1437–1448.
76. Blazejewska AI, Schwarz ST, Pitiot A, Stephenson MC, Lowe J, Bajaj N, *et al.* Visualization of nigrosome 1 and its loss in PD: pathoanatomical correlation and *in vivo* 7 T MRI. *Neurology* 2013, 81: 534–540.
77. Massey LA, Miranda MA, Al-Helli O, Parkes HG, Thornton JS, So P-W, *et al.* 9.4 T MR microscopy of the substantia nigra with pathological validation in controls and disease. *Neuroimage Clin* 2017, 13: 154–163.
78. Damier P, Hirsch EC, Agid Y, Graybiel AM. The substantia nigra of the human brain. *Brain* 1999, 122: 1437–1448.
79. Schwarz ST, Mougin O, Xing Y, Blazejewska A, Bajaj N, Auer DP, *et al.* Parkinson's disease related signal change in the nigrosomes 1–5 and the substantia nigra using T2\* weighted 7T MRI. *Neuroimage Clin* 2018, 19: 683–689.
80. Zarow C, Lyness SA, Mortimer JA, Chui HC. Neuronal loss is greater in the locus coeruleus than nucleus basalis and substantia nigra in Alzheimer and Parkinson diseases. *Arch Neurol* 2003, 60: 337–341.
81. Vazey EM, Aston-Jones G. The emerging role of norepinephrine in cognitive dysfunctions of Parkinson's disease. *Front Behav Neurosci* 2012, 6: 48.
82. Keren NI, Taheri S, Vazey EM, Morgan PS, Granholm ACE, Aston-Jones GS, *et al.* Histologic validation of locus coeruleus MRI contrast in post-mortem tissue. *Neuroimage* 2015, 113: 235–245.
83. Birkl C, Langkammer C, Golob-Schwarzl N, Leoni M, Haybaeck J, Goessler W, *et al.* Effects of formalin fixation and temperature on MR relaxation times in the human brain. *NMR Biomed* 2016, 29: 458–465.
84. Shatil AS, Uddin MN, Matsuda KM, Figley CR. Quantitative Ex Vivo MRI changes due to progressive formalin fixation in whole human brain specimens: longitudinal characterization of diffusion, relaxometry, and myelin water fraction measurements at 3T. *Front Med* 2018, 5: 31.
85. Prouvoulos N, Jacobs HIL, Ivanov D, Uludağ K, Verhey FRJ, Poser BA. High-resolution *in vivo* imaging of human locus coeruleus by magnetization transfer MRI at 3T and 7T. *Neuroimage* 2018, 168: 427–436.
86. Jones NR, Blumbergs PC, Brown CJ, McLean AJ, Manavis J, Perrett LV, *et al.* Correlation of postmortem MRI and CT appearances with neuropathology in brain trauma: a comparison of two methods. *J Clin Neurosci* 1998, 5: 73–79.
87. Hesselink JR, Dowd CF, Healy ME, Hajek P, Baker LL, Luerssen TG. MR imaging of brain contusions: a comparative study with CT. *AJR Am J Roentgenol* 1988, 150: 1133–1142.
88. Vilela P, Rowley HA. Brain ischemia: CT and MRI techniques in acute ischemic stroke. *Eur J Radiol* 2017, 96: 162–172.
89. Milidonis X, Marshall I, Macleod MR, Sena ES. Magnetic resonance imaging in experimental stroke and comparison with histology. *Stroke* 2015, 46: 843–851.
90. Knight MJ, McGarry BL, Rogers HJ, Jokivarsi KT, Gröhn OH, Kauppinen RA. A spatiotemporal theory for MRI T<sub>2</sub> relaxation time and apparent diffusion coefficient in the brain during acute ischaemia: application and validation in a rat acute stroke model. *J Cereb Blood Flow Metab* 2016, 36: 1232–1243.

91. Holleran L, Kim JH, Gangolli M, Stein T, Alvarez V, McKee A, *et al.* Axonal disruption in white matter underlying cortical sulcus tau pathology in chronic traumatic encephalopathy. *Acta Neuropathol* 2017, 133: 367–380.
92. Ruprecht R, Scheurer E, Lenz C. Systematic review on the characterization of chronic traumatic encephalopathy by MRI and MRS. *J Magn Reson Imaging* 2019, 49: 212–228.
93. Yelnik J, Bardinet E, Dormont D, Malandain G, Ourselin S, Tandé D, *et al.* A three-dimensional, histological and deformable atlas of the human basal ganglia. I. Atlas construction based on immunohistochemical and MRI data. *Neuroimage* 2007, 34: 618–638.
94. Chakravarty MM, Bertrand G, Hodge CP, Sadikot AF, Collins DL. The creation of a brain atlas for image guided neurosurgery using serial histological data. *Neuroimage* 2006, 30: 359–376.
95. Cardinale F, Chinnici G, Bramerio M, Mai R, Sartori I, Cossu M, *et al.* Validation of FreeSurfer-estimated brain cortical thickness: comparison with histologic measurements. *Neuroinformatics* 2014, 12: 535–542.
96. Morel A, Magnin M, Jeanmonod D. Multiarchitectonic and stereotactic atlas of the human thalamus. *J Comp Neurol* 1997, 387: 588–630.
97. Gaugler JE, Ascher-Svanum H, Roth DL, Fafowora T, Siderowf A, Beach TG. Characteristics of patients misdiagnosed with Alzheimer’s disease and their medication use: an analysis of the NACC-UDS database. *BMC Geriatr* 2013, 13: 137.
98. Rizzo G, Copetti M, Arcuti S, Martino D, Fontana A, Logroscino G. Accuracy of clinical diagnosis of Parkinson disease. *Neurology* 2016, 86: 566–576.
99. Yan F, He N, Lin H, Li R. Iron deposition quantification: applications in the brain and liver. *J Magn Reson Imaging* 2018, 48: 301–317.
100. Yoo Y, Tang LYW, Brosch T, Li DKB, Kolind S, Vavasour I, *et al.* Deep learning of joint myelin and T1w MRI features in normal-appearing brain tissue to distinguish between multiple sclerosis patients and healthy controls. *Neuroimage Clin* 2018, 17: 169–178.
101. Ambastha AK, Leong TY, Alzheimer’s Disease Neuroimaging Initiative. A deep learning approach to neuroanatomical characterisation of Alzheimer’s disease. *Stud Health Technol Inform* 2017, 245: 1249.
102. Jonkman LE, Fleysher L, Steenwijk MD, Koeleman JA, de Snoo TP, Barkhof F, *et al.* Ultra-high field MTR and qR2\* differentiates subpial cortical lesions from normal-appearing gray matter in multiple sclerosis. *Mult Scler* 2016, 22: 1306–1314.
103. Derakhshan M, Caramanos Z, Narayanan S, Arnold DL, Louis Collins D. Surface-based analysis reveals regions of reduced cortical magnetization transfer ratio in patients with multiple sclerosis: a proposed method for imaging subpial demyelination. *Hum Brain Mapp* 2014, 35: 3402–3413.
104. Oguz I, Yaxley R, Budin F, Hoogstoel M, Lee J, Maltbie E, *et al.* Comparison of magnetic resonance imaging in live vs. post mortem rat brains. *PLoS One* 2013, 8: e71027.
105. Scheurer E, Lovblad KO, Kreis R, Maier SE, Boesch C, Dirnhofer R, *et al.* Forensic application of postmortem diffusion-weighted and diffusion tensor MR imaging of the human brain in situ. *Am J Neuroradiol* 2011, 32: 1518–1524.
106. Braak H, Braak E. Neuropathological staging of Alzheimer-related changes. *Acta Neuropathol* 1991, 82: 239–259.
107. Ikonomic MD, Klunk WE, Abrahamson EE, Mathis CA, Price JC, Tsopoulos ND, *et al.* Post-mortem correlates of *in vivo* PiB-PET amyloid imaging in a typical case of Alzheimer’s disease. *Brain* 2008, 131(Pt 6): 1630–1645.